Biochem. J. (2013) **449**, 649–659 (Printed in Great Britain) doi:10.1042/BJ20120506





# Molecular mechanisms underlying the interaction of protein phosphatase-1c with ASPP proteins

Tamara D. SKENE-ARNOLD*, Hue Anh LUU*, R. Glen UHRIG†, Veerle DE WEVER†, Mhairi NIMICK†, Jason MAYNES‡, Andrea FONG*, Michael N. G. JAMES*, Laura TRINKLE-MULCAHY§, Greg B. MOORHEAD† and Charles F. B. HOLMES*[1]

*Department of Biochemistry, 3-37 Medical Sciences Building, School of Translational Medicine, Faculty of Medicine and Dentistry, University of Alberta, Edmonton, Canada, T6G 2H7, †Department of Biological Sciences, University of Calgary, Calgary, Toronto, Canada, T2N 1N4, ‡Department of Paediatric Anaesthesia and Molecular Structure and Function, Hospital for Sick Children/SickKids Research Institute, Faculty of Medicine, University of Toronto, AB, ON, Canada, M5G 1X8, and §Department of Cellular and Molecular Medicine, University of Ottawa, Ottawa, ON, Canada, KIH 8MS

The serine/threonine PP-1c (protein phosphatase-1 catalytic subunit) is regulated by association with multiple regulatory subunits. Human ASPPs (apoptosis-stimulating proteins of p53) comprise three family members: ASPP1, ASPP2 and iASPP (inhibitory ASPP), which is uniquely overexpressed in many cancers. While ASPP2 and iASPP are known to bind PP-1c, we now identify novel and distinct molecular interactions that allow all three ASPPs to bind differentially to PP-1c isoforms and p53. iASPP lacks a PP-1c-binding RVXF motif; however, we show it interacts with PP-1c via a RARL sequence with a $K_d$ value of 26 nM. Molecular modelling and mutagenesis of PP-1c–ASPP protein complexes identified two additional modes of interaction. First, two positively charged residues, $Lys^{260}$ and $Arg^{261}$ on PP-1c, interact with all ASPP family members. Secondly, the C-terminus of the PP-1c $\alpha$, $\beta$ and $\gamma$ isoforms contain a type-2 SH3 (Src homology 3) poly-proline motif (PxxPxR), which binds directly to the SH3 domains of ASPP1, ASPP2 and iASPP. In PP-1c$\gamma$ this comprises residues 309–314 (PVTPPR). When the Px(T)PxR motif is deleted or mutated via insertion of a phosphorylation site mimic (T311D), PP-1c fails to bind to all three ASPP proteins. Overall, we provide the first direct evidence for PP-1c binding via its C-terminus to an SH3 protein domain.

Key words: apoptosis-stimulating protein of p53 (ASPP), protein phosphatase-1 catalytic subunit (PP-1c), protein–protein interaction, RVXF-binding motif, Src homology 3 domain (SH3 domain).

## INTRODUCTION

Nearly 70% of all eukaryotic proteins are modified by reversible phosphorylation reactions [1]. While the human genome encodes for approximately 400 serine/threonine protein kinases, it encodes for substantially fewer serine/threonine protein phosphatase catalytic subunits, as protein kinases outnumber protein phosphatases by three to one [2]. A key biological question is how a small number of protein phosphatases can counteract the actions of many protein kinases to maintain spatial and temporal regulation of substrate dephosphorylation. In mammals, there are three isoforms of the type-1 protein phosphatase PP-1c (protein phosphatase-1 catalytic subunit; $\alpha$, $\beta$ and $\gamma$) that share 76–88% sequence identity, differing mainly within their N- and C-termini. PP-1c associates with multiple R-subunits (regulatory subunits), which target PP-1c to specific substrates to balance the actions of serine/threonine protein kinases. To date, over 180 PP-1c R-subunits have been identified [3,4]. By binding to R-subunits, PP-1c exists in many different mutually exclusive oligomeric states within a cell, altering not only its substrate specificity, but also targeting to specific subcellular locations.

PP-1c R-subunits interact with PP-1c through multiple contact sites [5,6]; however, the majority of PP-1c regulatory proteins contain a conserved amino acid consensus sequence referred to as the RVXF-binding motif ([K/R]-$X_{0-1}$-[V/I/L]-X-[F/W], where X can be any amino acid except proline). This motif binds to PP-1c in an extended fashion within a hydrophobic pocket of PP-1c remote from the catalytic site [7,8]. Mutation of hydrophobic valine and phenylalanine positions in the motif abolishes the ability of full-length R-subunits to bind to PP-1c [7–9]. Additionally, short synthetic RVXF-containing peptides competitively bind to PP-1c and are sufficient to disrupt the binding of RVXF-containing R-subunits [7,8,10].

The ankyrin-repeat, SH3 (Src homology 3) domain and proline-rich region containing proteins are a unique family of p53-binding proteins that modulate the activity of p53 [11]. Therefore, they are often referred to as the ASPPs (apoptosis-stimulating proteins of p53). The human genome encodes three principal ASPP proteins: ASPP1, ASPP2 and an iASPP (inhibitory ASPP; Figure 1). ASPP2 was found to be homologous with two other proteins, later named ASPP1 and iASPP [11]. ASPP1 and ASPP2 bind directly to the DNA-binding domain of wild-type p53 via their ankyrin-repeat and SH3 domains to enhance the apoptotic function of p53 [12,13]. The crystal structure of p53 bound to p53BP2/ASPP2 revealed that ASPP2 binds to the same region of p53 that interacts with DNA [14,15]. Not surprisingly, mutants of p53 commonly found in cancer lack the ability to interact with DNA or ASPP2 [16]. Although iASPP also interacts with the DNA-binding domain of p53, unlike ASPP1 and ASPP2, iASPP was shown to also bind with higher affinity to the N-terminal proline-rich domain of p53 [12]. Differences in binding to p53 may provide one explanation of how ASPP1/2 and iASPP have opposing functions within the cell.

Abbreviations used: ASPP, apoptosis-stimulating proteins of p53; $\beta$-Me, 2-mercaptoethanol; CDK2, cyclin-dependent kinase 2; DTT, dithiothreitol; GFP, green fluorescent protein; iASPP, inhibitory ASPP; HCC, hepatocellular carcinoma; IP, immunoprecipitation; IPTG, isopropyl $\beta$-D-thiogalactopyranoside; LB, Luria–Bertani; MC, microcystin; NF-$\kappa$B, nuclear factor $\kappa$B; Ni-NTA, $Ni^{2+}$-nitrilotriacetate; pNPP, *p*-nitrophenyl phosphate; PP-1c, protein phosphatase-1 catalytic subunit; hPP-1c, human PP-1c; R-subunit, regulatory subunit; SH3, Src homology 3; SILAC, stable isotope by amino acid labelling in culture.

[1] To whom correspondence should be addressed (email Charles.holmes@ualberta.ca).

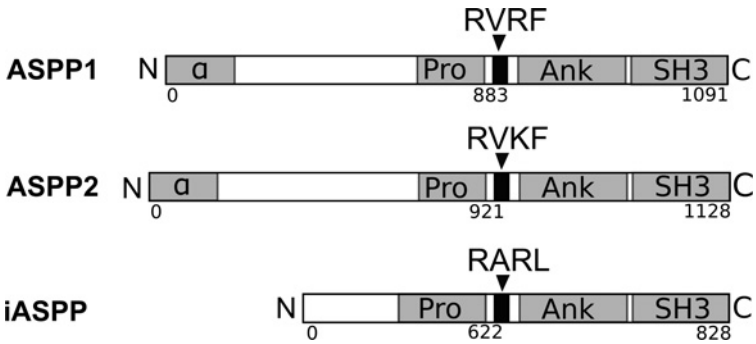


**Figure 1 Linear domain structures of the ASPPs**

Both ASPP1 and ASPP2 contain a canonical PP-1c-binding motif (RVRF and RVKF respectively), whereas iASPP contains an RVXF-like motif (RARL). Regions in the ASPP proteins are depicted as: $\alpha$, $\alpha$-helical domain; Pro, proline-rich-region; Ank, ankyrin-repeat; and SH3, Src-homology 3 (SH3) domain.

iASPP was originally identified as RAI [inhibitor of the RelA p65 subunit of NF-$\kappa$B (nuclear factor $\kappa$B)] [17]. iASPP is conserved from worms to humans and, unlike ASPP1 and ASPP2, functions as an oncogene in cells by decreasing the apoptotic activity of p53. iASPP is overexpressed in many cancers that typically have normal levels of ASPP2 and p53, including breast cell carcinomas and acute myeloid leukaemias [12,13,18]. Additionally, iASPP and p53 were shown to form a negative-feedback loop, as iASPP protein expression is induced indirectly through the accumulation and activation of p53 [19]. The C-terminus of iASPP (ankyrin-repeat and SH3 domains) is homologous with the C-termini of ASPP1 and ASPP2, and iASPP has been shown to directly compete with ASPP1 and ASPP2 for binding to p53 [20].

ASPP1 and ASPP2 were later shown to bind to other proteins, including the p65 subunit (RelA) of NF-$\kappa$B, the hepatitis C virus core protein, Bcl-2, YAP (Yes-associated protein), Lats2 (large tumour suppressor protein 2) and PP-1c [21–27]. ASPP2 contains a principal PP-1c RVXF binding motif and has been shown to bind to PP-1c with a greater affinity than p53 [27]. ASPP1 also contains an equivalent RVXF motif and therefore prior to the present study we predicted it would also bind to PP-1c. In contrast, although iASPP retains its ability to bind to p53, it does not contain a classical PP-1c RVXF motif. Nevertheless, Llanos et al. [28] have shown that iASPP is able to bind to PP-1c. In the present study, we have investigated the molecular interactions between ASPP proteins and PP-1c. We demonstrate that both ASPP1 and iASPP have the ability to bind to PP-1c in a stable 1:1 complex and these protein complexes are disrupted by the addition of RVXF-containing peptides. Furthermore, by using molecular modelling and site-specific mutagenesis we have identified several unique regions of PP-1c that are essential for interaction with the ASPP proteins.

## EXPERIMENTAL

### Materials

The active-site-directed protein phosphatase inhibitor, MC (microcystin)-LR, was purified from *Microcystis aeruginosa* collected from Little Beaver Lake (Ferintosh, AB, Canada) as described previously [29]. Full-length human wild-type cDNA for ASPP2 (GenBank® accession number NM_005426) and iASPP (GenBank® accession number NM_006663) were used as described previously [12]. Full-length ASPP1 cDNA (GenBank® accession number NM_015316) was prepared as described in [30]. Full-length ASPP2 and iASPP cDNA constructs were provided by Dr Xin Lu (Ludwig Institute for Cancer Research, Oxford, U.K.) [28]. Full-length human p53 cDNA (GenBank® accession number NM_000546) was purchased from B-Bridge International. Unless otherwise stated, all other chemicals and reagents were purchased from Sigma–Aldrich. MC–Sepharose and control Sepharose preparations were synthesized as described previously [31,32]. Affinity-displacement chromatography and co-IP (immunoprecipitation) experiments were carried out as described in Moorhead et al. [33].

### Expression and purification of recombinant PP-1c isoforms

Human and rabbit recombinant PP-1c isoforms $\alpha$, $\beta$ and $\gamma$ (GenBank® accession numbers NM_001008709, XM_002719749 and NM_001244974 respectively) were expressed and purified to homogeneity as described in [34], with the following modifications. A single colony of *Escherichia coli* C41 DE3 cells transformed with either pKK223.3-hPP-1c$\alpha$, pCW-rPP-1c$\beta$ or pCW-hPP-1c$\gamma$ was used to inoculate a 400 ml overnight culture of LB (Luria–Bertani) medium containing 1 mM $MnCl_2$ and 200 $\mu$g/ml ampicillin. The overnight culture was then subcultured into 4 litres of LB medium containing 1 mM $MnCl_2$, 0.001 % vitamin $B_1$ and 200 $\mu$g/ml ampicillin. Once the culture reached an attenuance of approximately 0.5 at 600 nm, protein expression was induced with 0.1–0.5 mM IPTG (isopropyl $\beta$-D-thiogalactopyranoside) for 18 h. Cells were harvested by centrifugation at 6000 ***g*** for 45 min and 4 °C and resuspended in approximately 130 ml of buffer A [50 mM imidazole (pH 7.5), 0.5 mM EDTA, 0.5 mM EGTA, 2 mM $MnCl_2$, 0.5 mM PMSF, 2 mM benzamidine, 3 mM DTT (dithiothreitol), 100 mM NaCl and 10 % (v/v) glycerol] containing 2 $\mu$g/$\mu$l DNase A and one SigmaFAST™ protease inhibitor tablet. Cells were then lysed by three consecutive passes through an Emulsiflex-C3 high-pressure homogenizer (Avestin) and centrifuged for 45 min at 13 000 ***g*** at 4 °C. Supernatant was loaded on to a heparin–Sepharose CL-6B column (GE Healthcare) and PP-1c protein was eluted using a 400 ml linear gradient of buffer A containing 0.1–0.5 M NaCl. Fractions were assayed for phosphatase activity using the colorimetric pNPP (*p*-nitrophenyl phosphate) assay [35,36]. Active fractions were pooled and diluted 3.5× in buffer B [50 mM imidazole (pH 7.5), 0.5 mM EDTA, 2 $MnCl_2$, 2 mM DTT and 20 % (v/v) glycerol], loaded on to a human Inhibitor-2 (I-2) affinity column and eluted in buffer B containing 1 M NaCl. Active fractions, confirmed to be homogeneously pure by SDS/PAGE (12 % gel) analysis, were pooled and concentrated to 1–4 mg/ml, an equal volume of glycerol added, and stored at − 20 °C.

### Expression and purification of human recombinant His-tagged ASPP and p53 constructs

ASPP1$^{867–1090}$, ASPP2$^{905–1128}$, iASPP$^{608–828}$, iASPP$^{626–828}$ and p53$^{2–293}$ constructs were generated using PCR amplification, engineering unique 3′ and 5′ restriction enzyme cleavage sites (EcoRI and XhoI respectively). The iASPP$^{608–828}$ L625A mutant was generated using QuikChange® site-directed mutagenesis, as described for PP-1c mutants. Each construct was cloned into the pET28A vector and transformed into *E. coli* Rosetta pLys cells (Novagen). A single colony of *E. coli* Rosetta cells transformed with a plasmid construct was used to inoculate 400 ml of LB medium containing chloramphenicol (34 $\mu$g/ml) and kanamycin (30 $\mu$g/ml). After cell growth overnight at 37 °C, the culture was used to inoculate 4 litres of LB medium containing chloramphenicol (34 $\mu$g/ml) and kanamycin (30 $\mu$g/ml) and were grown at 37 °C to an attenuance of 0.5 at 600 nm. Protein expression was induced with 0.1 – 0.3 mM IPTG for 18 h at 28 °C. The cells were harvested by centrifugation at 4 °C for 15 min at 6000 ***g***. Pelleted cells were resuspended in 150 ml of buffer F [25 mM sodium phosphate (pH 8.0), 125 mM NaCl and 1 % (v/v) Tween 20] containing 15 mM imidazole, 2.7 mM KCl, 1 mM PMSF, 1.5 ml of protease inhibitor cocktail for His-tagged proteins (Sigma), and 5 mM $\beta$-Me (2-mercaptoethanol). Cells were lysed as described for PP-1c and centrifuged for 45 min at 13 000 ***g*** at 4 °C. Supernatant was applied to a Ni-NTA ($Ni^{2+}$-nitrilotriacetate) affinity His-prep FF 16/10 column (GE Healthcare) at 1.0 ml · $min^{-1}$. ASPP proteins were eluted in buffer F containing 250 mM imidazole. Elution fractions (5 ml) were pooled based on SDS/PAGE (12 % gel) analysis and then separated on a Superdex 75 26/60 size-exclusion column (GE Healthcare), at 0.9 ml · $min^{-1}$. Protein was eluted with buffer G [25 mM Tris/HCl (pH 8.0), 150 mM NaCl and 1 mM DTT] as described previously [37]. Fractions (3 ml) were pooled based on SDS/PAGE (12 % gel) analysis and concentrated to ∼5 mg/ml. An equal amount of glycerol was added and the solution stored at − 20 °C.

### Gel-filtration chromatography binding experiments

Gel-filtration chromatography was performed using FPLC (Amersham Pharmacia Biotech). Highly purified preparations of PP-1c$\alpha$ and His-tagged iASPP$^{608–828}$ were incubated either alone or together at 30 °C for 45 min prior to resolution on a Superdex 75 10/30 gel-filtration column (GE Healthcare). The proteins were resolved at a flow rate of 0.1 ml · $min^{-1}$ using buffer H [50 mM imidazole (pH 7.8), 0.3 M NaCl, 0.5 mM EDTA, 0.5 mM EGTA, 2.0 mM DTT and 10 % glycerol] containing 2 mM $MnCl_2$. Fractions (250 $\mu$l) were collected and analysed by SDS/PAGE (12 % gel).

For the trimeric binding studies involving PP-1c, ASPPs and p53, gel filtration was performed as described above in the presence or absence of p53$^{2–293}$. Fractions were assayed for protein phosphatase activity using the pNPP assay [36] and analysed by SDS/PAGE (12 % gel) with Coomassie Blue staining.

### Ni-NTA affinity chromatography binding experiments

Approximately 20$\mu$l of Ni-NTA agarose (Qiagen) was incubated end-over-end for 1 h at 4 °C with 5 $\mu$g of either ASPP1$^{867–1090}$, ASPP2$^{905–1128}$ or iASPP$^{608–828}$, reconstituted in 300 $\mu$l of buffer I [25 mM Tris/HCl (pH 7.5), 10 mM imidazole, 150 mM NaCl and 0.5 mM $MnCl_2$]. Ni-NTA resin was washed with buffer J [25 mM Tris/HCl (pH 7.5), 30 mM imidazole, 500 mM NaCl, 0.5 mM $MnCl_2$ and 0.1 % Tween 20] until no further protein could be eluted. Wild-type or mutant PP-1c (∼5 $\mu$g) was diluted in buffer J and incubated with bound Ni-NTA resin at 4 °C for 1–18 h. After washing, protein was eluted from the resin by boiling samples in 30 $\mu$l of 2× SDS/PAGE loading buffer [65 mM Tris/HCl (pH 6.8), 26 % (v/v) glycerol, 2 % (w/v) SDS and 0.1 % Bromophenol Blue] at 100 °C for 5 min. Samples were then analysed by SDS/PAGE (12 % gel).

### Annotation of ASPP family members in cytoplasmic interactomes of PP-1c$\alpha$ and PP-1c$\gamma$

Quantitative SILAC (stable isotope by amino acid labelling in culture)-based mass spectrometric analysis of immunopurified PP-1c complexes was carried out on cytoplasmic extracts from HeLa cells stably expressing low levels of GFP (green fluorescent protein)–PP-1c$\alpha$ or GFP–PP-1c$\gamma$, using a similar approach to previously published nuclear interactome screens [38,39]. Briefly, cells were labelled for >5 days with medium containing heavy isotopes of the essential amino acids arginine and lysine, for complete incorporation into all proteins. An IP of GFP–PP-1c from a cellular extract was compared directly with an IP from cells not expressing the fusion protein, with the affinity matrices combined for protein elution and all subsequent steps, including separation by one-dimensional SDS/PAGE (to reduce complexity) and identification of all eluted proteins by MS. Quantification of the level of heavy/light arginine and lysine in each peptide yields a 'SILAC ratio' that reveals whether a protein bound non-specifically to the affinity matrix in both IPs (ratio ∼1:1) or was specifically enriched with GFP–PP-1c (ratio >1). MaxQuant quantitative proteomics software (http://www.maxquant.org) was used for protein identification, quantification of the SILAC ratios and calculation of summed peptide intensities for comparison of relative abundance.

### Determination of the activity of PP-1c$\gamma$ and PP-1c$\gamma$ mutants after phosphorylation by the protein kinase cyclin A–CDK2 (cyclin-dependent kinase 2)

Purified recombinant hPP-1c$\gamma$ (human PP-1c$\gamma$) was phosphorylated with cyclin A–CDK2 (100 units/$\mu$l; New England Biolabs). The final concentrations for the reagents in the phosphorylation reaction were as follows: hPP-1c$\gamma$ (0.14 $\mu$g/$\mu$l), 0.2 mM [$\gamma$-$^{32}$P]ATP, 40 mM Tris/HCl (pH 7.5), 10 mM $MgCl_2$, 5 mM $MnCl_2$ and 2 mM DTT. Cyclin A–CDK2 (400 units) was used to phosphorylate hPP-1c$\gamma$ in a 30 $\mu$l assay mixture. Phosphorylation was performed at 30 °C. Samples (2 $\mu$l) were removed from the reaction at 0, 5, 10, 20, 30 and 45 min and added to an appropriate volume of buffer K [50 mM Tris/HCl (pH 7), 0.1 mM EDTA, 1 mg/ml BSA, 0.2 % $\beta$-Me and 8 mM $MnCl_2$] to give approximately 15 % $^{32}$P release from [$^{32}$P]phosphorylase *a* at time point zero [40]. [$^{32}$P]Phosphorylase *a* was prepared as described previously [41].

## RESULTS AND DISCUSSION

In the present study we characterized the distinct molecular interaction mechanisms of two newly identified PP-1c-binding proteins, ASPP1 and iASPP. We have shown that both proteins bind directly to the catalytic subunit of PP-1c, forming stable 1:1 complexes. These interactions occur *in vivo*, as demonstrated by SILAC, a non-biased approach in which PP-1c was affinity-purified and interacting partners identified by quantitative MS.

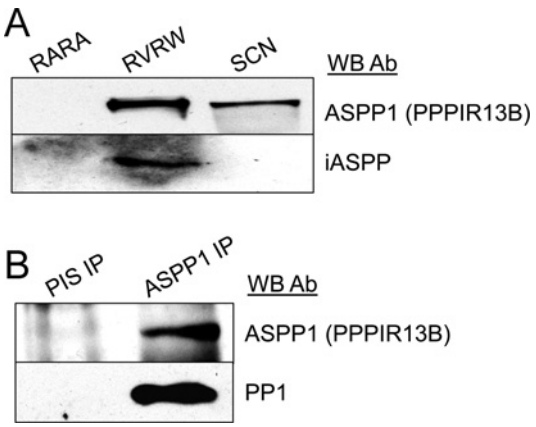


**Figure 2 Displacement affinity chromatography identifies ASPP–PP-1c and iASPP–PP-1c complexes from HeLa cell lysate**

(**A**) HeLa cell lysate was incubated with MC–Sepharose, washed and eluted sequentially using peptides containing a generic mutated GKKRARAADLE (RARA) and the wild-type (RVRW) GKKRVRWADLE PP-1c docking motif as described in [33]. The sodium thiocyanate (SCN) lane represents elution with 3 M sodium thiocyanate. All fractions were concentrated to an equal volume, run on 4–12 % SDS/PAGE (Invitrogen), immunoblotted and probed with antibodies (Ab) specific against ASPP1 and iASPP. (**B**) Co-IP of PP-1c from HeLa cell lysate using antibodies specific against ASPP1. IPs from HeLa cell lysates were performed using antibodies specific against ASPP1. Immunoprecipitated proteins were run on SDS/PAGE and probed with antibody against ASPP1 and an anti-(pan PP-1c) antibody. A pre-immune serum (PIS) control was performed in parallel. WB, Western blot.

### Identification of ASPP1 as a PP-1c regulatory protein

ASPP1, ASPP2 and iASPP are significantly homologous within their C-terminal domains and multiple sequence alignment reveals that both ASPP1 and ASPP2 contain an RVXF motif (RVRF, residues 883–886 and RVKF, residues 921–924 respectively). We predicted that ASPP1 would interact with PP-1c via its classical RVXF motif in a similar manner to ASPP2. The equivalent motif in the iASPP protein is RARL (residues 622–625) and previous mutational studies [7,8] have demonstrated the importance of the valine and phenylalanine residues in the RVXF motif. In addition, Llanos et al. [28] have shown that iASPP does interact directly with PP-1c and can bind in the absence of its RARL motif.

We carried out MC–Sepharose affinity chromatography, a technique that has been used successfully to identify novel PP-1c R-subunits [33]. Using MC–Sepharose, PP-1c is immobilized via its active site leaving the hydrophobic RVXF-interacting groove exposed; therefore MC–Sepharose can pull down many different multi-protein PP-1c complexes from a complex cellular lysate. HeLa cell lysate was incubated with MC–Sepharose, washed and eluted sequentially using peptides containing a generic mutated GKKRARAADLE (RARA) and a wild-type GKKRVRWADLE (RVRW) PP-1c docking motif as described previously [33]. Elutions were analysed by SDS/PAGE, immunoblotted and then probed with antibodies specific against ASPP1 and iASPP. The results of the present study show that ASPP1 does interact with endogenous HeLa cell PP-1c and is successfully eluted from the MC–Sepharose resin with the RVRW peptide, but not the generic mutated RARA peptide (Figure 2A). Subsequent addition of SCN (sodium thiocyanate) eluted additional ASPP1 from the MC–Sepharose resin, suggesting there may be additional interaction sites that stabilize the ASPP1–PP-1c complex. These initial experiments were corroborated by co-IP experiments performed with antibodies specific against ASPP1. Immunoprecipitated proteins were analysed by SDS/PAGE and probed with either the anti-ASPP1 antibody or an anti-(pan PP-1c) antibody (Figure 2B).

### iASPP is a novel PP-1c-interacting protein

Our initial displacement affinity chromatography experiments confirmed that iASPP also binds to PP-1c (Figure 2A). Interaction between iASPP and PP-1c is completely disrupted by the addition of a synthetic RVXF-containing peptide, indicating that iASPP binds to or near the hydrophobic RVXF-binding pocket of PP-1c. In order to further investigate the molecular interactions between PP-1c and ASPP proteins, a His-tagged construct of iASPP (iASPP$^{608–828}$) was created by PCR amplification. The equivalent ASPP1 and ASPP2 constructs (ASPP1$^{867–1090}$ and ASPP2$^{905–1128}$ respectively) were also made, which were designed to include the PP-1c RVXF motif of ASPP2 (Figure 1, RVKF, residues 921–924) and the corresponding motif in iASPP (RARL, residues 622–625). Gel-filtration chromatography was used to confirm that iASPP directly interacts with PP-1c. Purified preparations of PP-1c$\alpha$ and His-tagged iASPP$^{608–828}$ were incubated alone or together at 30 °C for 45 min prior to resolution on a Superdex 75 10/30 gel-filtration column. Fractions were then analysed by SDS/PAGE and Coomassie Blue staining. Alone, PP-1c$\alpha$ and iASPP$^{608–828}$ each elute as 37 kDa and 28 kDa monomers respectively (Figures 3A and 3B). After incubating PP-1c$\alpha$ with iASPP at 30 °C for 45 min, they eluted together as a stable 1:1 $\sim$60 kDa heterodimeric complex (Figure 3C), demonstrating that iASPP binds directly to PP-1c. When iASPP was run alone (Figure 3B), there was a small peak in fractions 36–38, which could indicate there is a small amount of the aggregated iASPP$^{608–828}$. However, SDS/PAGE of the gel-filtration fractions revealed that there was little to no iASPP protein in these fractions and alone the majority of the iASPP protein exists as an approximately 30 kDa monomer.

### iASPP protein binds to PP-1c via a non-classical motif

Since the results of the present study showed that iASPP binds directly with PP-1c and this interaction could be disrupted with a synthetic RVXF peptide (Figure 2A), this raised the idea that iASPP may have a hitherto unidentified binding motif. In order to test whether iASPP residues R$^{622}$ARL$^{625}$ function as a non-classical RVXF motif, we created two additional His-tagged iASPP constructs: an N-terminal truncation, iASPP$^{626–828}$, that lacks the RARL motif and a single point mutant iASPP$^{608–828}$ L625A. Ni-NTA affinity-binding experiments were carried out by comparing the binding of PP-1c$\alpha$ with wild-type iASPP$^{608–828}$, truncated iASPP$^{626–828}$ or mutated iASPP$^{608–828}$ L625A. These results show (Figure 3D) that both deletion of iASPP residues 608–625 or point mutation of L625A lessened the ability of iASPP to bind to PP-1c$\alpha$, indicating that RARL is a determinant for PP-1c docking. When combined with the fact that the iASPP–PP-1c complex is disrupted by the addition of synthetic RVXF-containing peptides (Figure 2A), this suggests that the iASPP RARL motif may be a functional, but degenerative, RVXF motif.

### ASPP proteins preferentially bind to the PP-1c$\alpha$ isoform

Previously, several key PP-1c regulatory proteins have exhibited selective binding to one PP-1c isoform ($\alpha$, $\beta$ or $\gamma$) over the others [5,38,42]. In order to test whether ASPP1, ASPP2 and/or iASPP selectively bind to a specific PP-1c isoform, we performed Ni-NTA pull downs, comparing the binding of PP-1c isoforms $\alpha$, $\beta$ and $\gamma$ to each of our His-tagged ASPP protein constructs (ASPP1$^{867–1090}$, ASPP2$^{905–1128}$ and iASPP$^{608–828}$). Our results show that all three ASPP proteins bind preferentially to PP-1c$\alpha$ (Figure 4). In this set of Ni-NTA-binding experiments, each phosphatase isoform was incubated with each ASPP construct for 45 min. When employing longer incubation times (over 5 h),

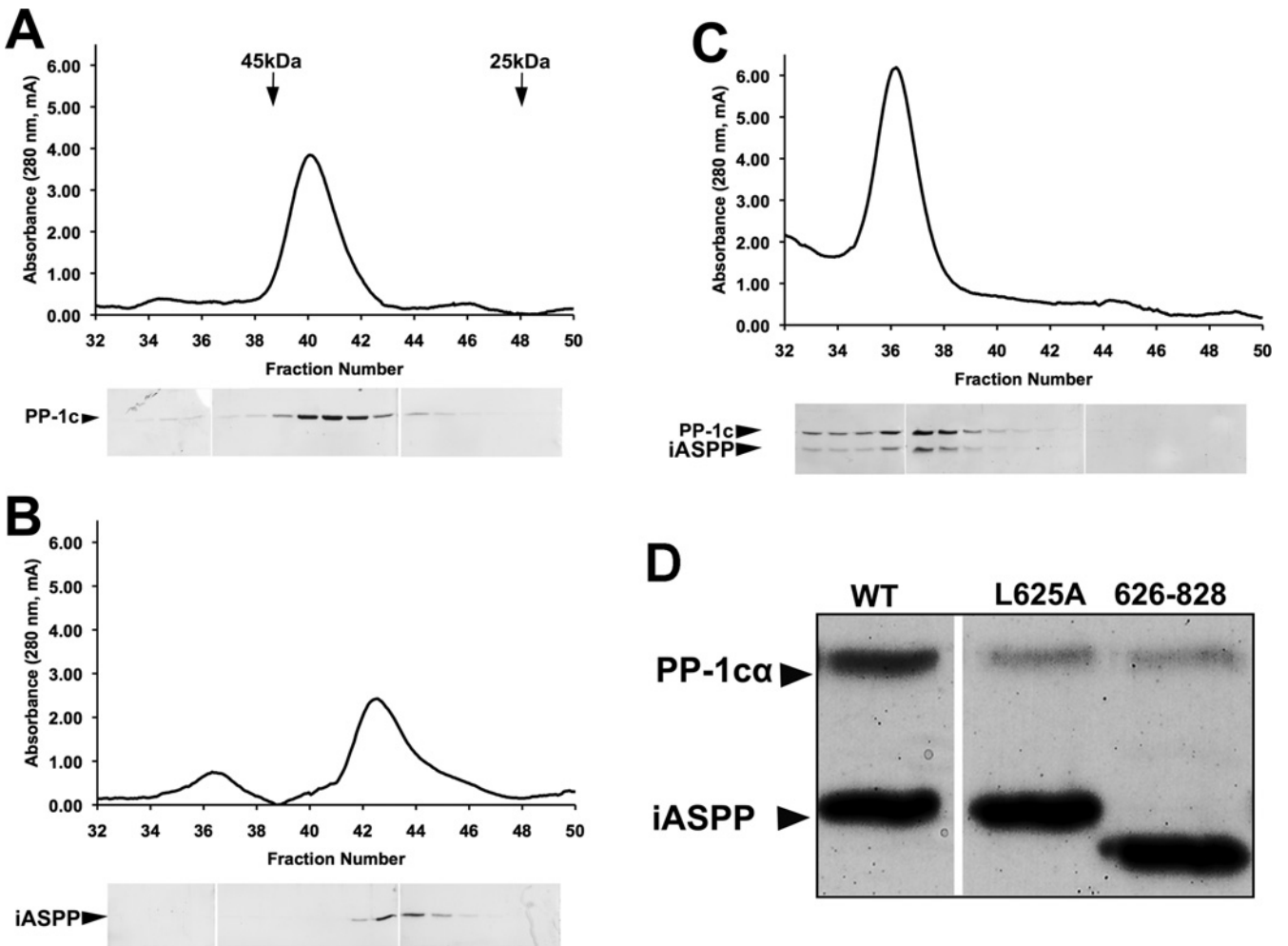


**Figure 3 Gel-filtration chromatography of protein phosphatase–ASPP complexes**

Gel-filtration chromatograph of PP-1c$\alpha$ alone (**A**), iASPP alone (**B**) and the PP-1c$\alpha$–iASPP$^{608–828}$ complex (**C**). Highly purified preparations of PP-1c$\gamma$ and His-tagged iASPP$^{608–828}$ were incubated either alone or together at 30 °C for 45 min prior to resolution on a Superdex 75 (10/30) gel-filtration column. The proteins were resolved at a flow rate of 0.1 ml/min using buffer H and 0.25 ml fractions collected for analysis by SDS/PAGE. SDS/PAGE analyses of fractions 33–49 (8.5–12.25 ml) are shown below each chromatograph. (**D**) *In vitro* Ni-NTA agarose-binding experiment, comparing the binding of wild-type (WT) iASPP$^{608–828}$, iASPP$^{608–828}$ L625A and iASPP$^{626–828}$ with PP-1c$\alpha$. iASPP$^{608–828}$ Leu$^{625}$ was mutated to an alanine residue to create the equivalent of a RARA motif in iASPP. Approximately 5 $\mu$g of each iASPP construct was bound to Ni-NTA resin for 1 h at 4 °C end-over-end. Resin was washed and 5 $\mu$g of PP-1c incubated with the resin for an additional 1 h at 4 °C. After sufficient washing, bound protein was eluted by the addition of SDS/PAGE loading buffer, heated at 100 °C for 5 mins and analysed by SDS/PAGE with Coomassie Blue staining.

all three PP-1c isoforms were capable of binding to each ASPP protein.

We also examined the enrichment of ASPP proteins in cytoplasmic pull downs of GFP-tagged PP-1c isoforms stably expressed in human cells. A comparison of the cytoplasmic GFP–PP-1c$\alpha$ interactome with the cytoplasmic GFP–PP-1c$\gamma$ interactome (with equivalent amounts of each tagged isoform recovered), using a quantitative SILAC MS-based proteomics approach [38,39], revealed that although all three ASPP family members co-precipitated with both isoforms, they were clearly more highly enriched and more abundant in the PP-1c$\alpha$ IP (Table 1).

### Identification of a novel region on PP-1c that mediates interactions with regulatory proteins

On the basis of the results described above, we created a structural model of the ASPP2–PP-1c holoenzyme complex (Figure 5A) using co-ordinates from the separately determined crystal structures of PP-1c$\beta$ [bound to the myosin phosphatase-targeting subunit (MYPT1)] and ASPP2 crystallized in complex with the DNA-binding domain of p53 [6,14]. Our model of the ASPP2–PP-1c complex predicts several key interactions between the phosphatase and the ASPP proteins. One potential interaction involves a positively charged patch on the surface of PP-1c (residues Lys$^{260}$ and Arg$^{261}$) and an acidic region of ASPP2 located within its first ankyrin-repeat (residues Glu$^{938}$ and Asp$^{940}$; Figure 5B). Sequence alignment of several key PP-1c regulatory proteins including the ASPP proteins (Figure 5C), reveals the presence of a common and conserved acidic motif 12–15 residues downstream of the RVXF motif. In order to test this hypothesis, we created three PP-1c$\alpha$ mutants (A259R, K260D and R261S) and tested their ability to bind to ASPP1$^{867–1090}$, ASPP2$^{905–1128}$ and iASPP$^{608–828}$ via Ni-NTA-binding experiments. Mutation of the PP-1c$\alpha$ residue A259R resulted in a robust increase in the amount of ASPP1, ASPP2 and iASPP that could bind to the phosphatase (Figure 5D). Mutation of either K260D or R261S reduced the ability of the ASPP proteins to bind by approximately 40 % and 70 % respectively.

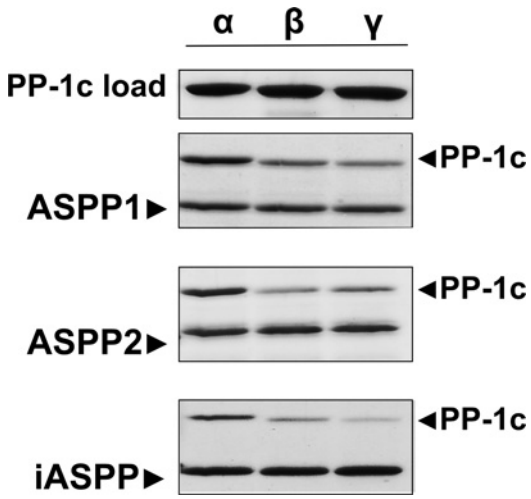


**Figure 4 ASPP proteins preferentially bind to the PP-1cα isoform**

The Figure depicts an *in vitro* Ni-NTA agarose pull-down experiment, comparing the binding of ASPP1$^{867–1090}$, ASPP2$^{905–1128}$ and iASPP$^{608–828}$ to PP-1c isoforms $\alpha$, $\beta$ and $\gamma$. Approximately 5 $\mu$g of each ASPP construct was bound to Ni-NTA for 1 h at 4 °C end-over-end. Resin was washed and 5 $\mu$g of PP-1c was added and incubated end-over-end for 45 min at 4 °C. After sufficient washing, protein was eluted by boiling samples in SDS/PAGE loading buffer and analysed by SDS/PAGE with Coomassie Blue staining.

This region of PP-1c is also important for interaction with other PP-1c-binding proteins including Inhibitor-2, a classical PP-1c inhibitory protein [43]. We show that mutation of either A259R or R261S disrupted the ability of His-tagged Inhibitor-2 to bind to PP-1c (Supplementary Figure S1C at http://www.biochemj.org/bj/449/bj4490649add.htm). Crystal structures of PP-1c bound to the MYPT1 or spinophilin, suggest that Arg$^{261}$ of PP-1c also interacts directly with Glu$^{54}$ and Glu$^{438}$ of MYPT1 and spinophilin respectively [6,44]. Together, the results of the present study highlight the importance of this PP-1c region in its ability to interact with residues surrounding the RVXF motif of at least two different PP-1c-interacting proteins.

### The PP-1c C-terminus contains a type-2 SH3-binding motif, PxxPxR, that is essential for binding to ASPP proteins

The crystal structure of PP-1c$\beta$ bound to the MYPT1 revealed that the C-terminal tail of PP-1c makes extensive contacts with the ankyrin-repeat domain of MYPT1 [6]. This is the first determined structure of PP-1c where the C-terminus is visible; the PP-1c C-terminal tail is highly flexible and is disordered within previous crystal structures. In fact, the tail of PP-1c within the MYPT1–PP-1c$\beta$ crystal structure is only visible up to residue 309 and the last 20 residues (309–327) are disordered. Our model of the ASPP2–PP-1c complex (Figure 5A) also suggests that there may be extensive interactions between the C-terminal tail of PP-1c and the ankyrin-repeat domain of all three ASPP proteins.

In order to test the importance of the C-terminal tail in the ASPP–PP-1c interaction, we created a PP-1c$\gamma$ C-terminal tail deletion mutant, PP-1c$\gamma^{1-300}$, (Figure 6A) and tested the ability of PP-1c$\gamma^{1-300}$ to bind to His-tagged ASPP1$^{867–1090}$, ASPP2$^{905–1128}$ and iASPP$^{608–828}$ using Ni-NTA affinity-binding experiments (Figure 7). Deletion of the C-terminal tail of PP-1c$\gamma$ completely disrupted its ability to bind to ASPP1$^{867–1090}$, ASPP2$^{905–1128}$ and iASPP$^{608–828}$, compared with the wild-type PP-1c$\gamma$.

Further inspection of the PP-1c C-terminal sequences (Figure 6A), reveals that all three human PP-1c isoforms contain a putative type-2 SH3-binding motif PxxPxR (PVTPPR in PP-1c$\gamma$, residues 309–314). Within this motif, PP-1c also contains a CDK2–cyclin A phosphorylation site (residues Thr$^{320}$ and Thr$^{311}$ in PP-1c$\alpha$ and PP-1c$\gamma$ respectively); both PP-1c$\alpha$ and PP-1c$\gamma$ have been shown to be stoichiometrically phosphorylated by CDK2–cyclin A and CDK2–cyclin B both *in vitro* and *in vivo* [45,46]. Phosphorylation of this threonine residue allows the C-terminal tail of PP-1c to fold back into the active site of PP-1c and inhibit catalytic activity and, over time, PP-1c is reactivated through autodephosphorylation. In the present study, we confirm that PP-1c$\gamma$ Thr$^{311}$ is robustly phosphorylated by CDK2–cyclin A *in vitro* (Figure 6B) and this phosphorylation event inhibits the enzymatic activity towards phosphorylase *a* (Figure 6C). Mutation of Thr$^{311}$ to an aspartate residue (T311D) abolished the ability of CDK2–cyclin A to phosphorylate PP-1c$\gamma$ and, surprisingly, did not cause auto-inhibition of PP-1c$\gamma$ (Figures 6B and 6C respectively). This allowed us to use the PP-1c$\gamma$ (T311D) mutant as an ideal choice to test the effect of a negative charge within the type-2 SH3-binding motif. Unlike the case for phosphorylated wild-type PP-1c$\gamma$, the C-terminus of the T311D PP-1 mutant would not be expected to fold back into the active site of PP-1c and would be accessible to interact with the ASPP proteins and there would be no issue of autodephosphorylation at this residue. We attempted a similar experiment with PP-1c$\alpha$; however, the T320D or T320E phosphomimic mutants were very poorly expressed. This also predicated the need to use PP-1c$\gamma$ truncation mutants in the binding studies with ASPP proteins above.

Since the ASPP proteins all contain an SH3 domain, this raised the question whether the PP-1c C-terminal PxxPxR SH3-binding motif interacts directly with the SH3 domain of ASPP proteins. Also, since the CDK2 phosphorylation site of PP-1c is located within the putative SH3 PxxPxR binding motif, this strongly suggested that phosphorylation of the PP-1c C-terminus may affect PP-1c binding to ASPP proteins. The

**Table 1 The ASPP proteins interact preferentially with PP-1cα *in vivo***

Equivalent amounts of GFP–PP-1c$\alpha$ and GFP–PP-1c$\gamma$ were recovered from the respective cell lines (relative abundance of 14.5 for PP-1c$\alpha$ and 16.2 for PP-1c$\gamma$), permitting a direct comparison of the enrichment of associated targeting subunits. The ratio of H/L indicates the enrichment of the heavy form of the protein (recovered in the GFP–PP-1c pull down) over the light form of the protein (recovered in the control pull down of GFP alone). Relative abundance measurements are based on summed peptide intensities and normalized to the molecular mass. The data for Repo-Man and Taperin are included for comparison, as these proteins have been previously demonstrated to show isoform specificity (for PP-1c$\gamma$ and PP-1c$\alpha$ respectively).

| Protein | Number of peptides co-purified with GFP–PP-1cα | Ratio of H/L | Relative abundance | Number of peptides co-purified with GFP–PP-1cγ | Ratio of H/L | Relative abundance |
|---|---|---|---|---|---|---|
| ASPP1 | 30 | 39.8 | 0.25 | 36 | 24.2 | 0.16 |
| ASPP2 | 43 | 43.4 | 0.92 | 30 | 21.7 | 0.105 |
| iASPP | 40 | 58.7 | 2.35 | 15 | 3.8 | 0.013 |
| Repo-Man | Not detected | Not detected | Not detected | 34 | 9.6 | 0.32 |
| Taperin | 14 | 13.1 | 0.1 | 2 | 3.6 | 0.004 |

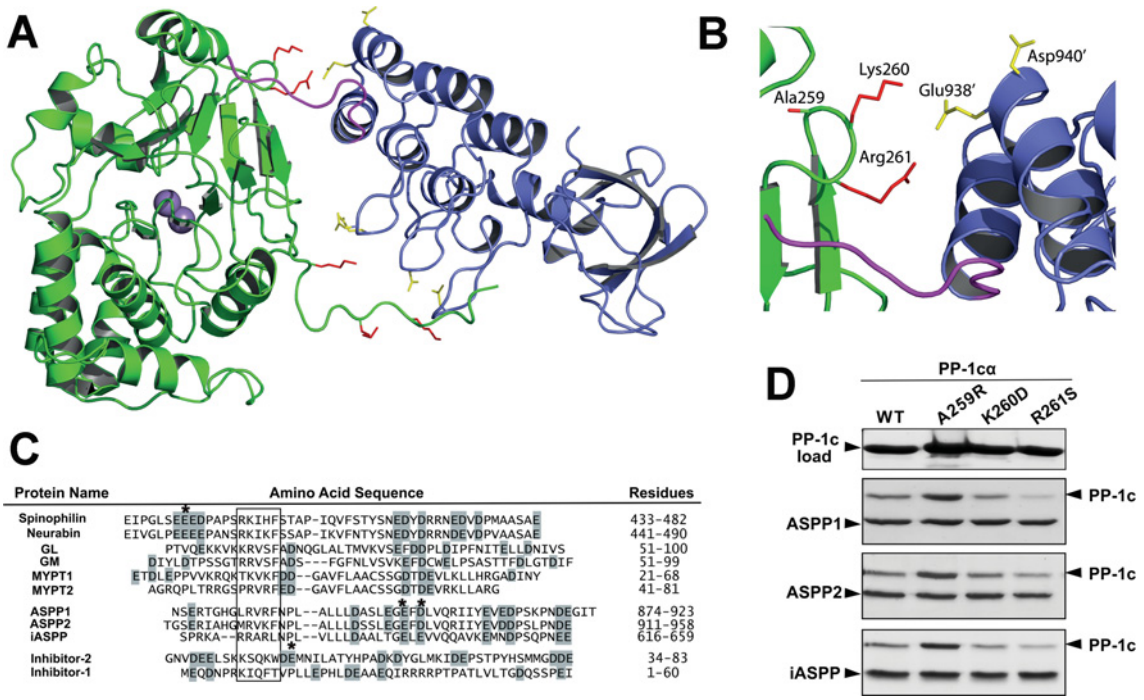


**Figure 5 PP-1c contains a positively charged region that is important for binding to the ASPP proteins**

(**A**) A structural model of the PP-1c–ASPP2 complex. The model, describing predicted interactions within this complex, was systematically constructed using co-ordinates from the separately determined crystal structures of PP-1c$\beta$ (PDB code 1S70) and a complex between p53 and ASPP2 (PDB code 1YCS) [6,14]. Ribbon representation: PP-1c$\beta$ (green) and ASPP2 (blue). Highlighted basic residues of PP-1c$\beta$ and acidic residues of ASPP2 are shown in red and orange respectively. (**B**) The predicted interactions between iASPP acidic residues Glu$^{938\prime}$ and Asp$^{940\prime}$ with two basic residues from PP-1c, Lys$^{260}$ and Arg$^{261}$. (**C**) An alignment of the PP-1c R-subunit sequences surrounding the canonical RVXF motif. The UniProt reference numbers for each regulatory protein are as follows: spinophilin, Q96SB3; neurabin, Q9ULJ8; glycogen-targeting subunit, liver form (GL), Q86XI6; glycogen-targeting subunit, muscle form (GM) Q16821; myosin phosphatase-targeting subunit-1 (MYPT1), O14974; myosin phosphatase-targeting subunit-2 (MYPT2), O60237; Inhibitor-1, Q13522; and Inhibitor-2, P41236. The RVXF motif of each PP-1c regulatory protein is outlined. The shaded grey box highlights a cluster of acidic residues C-terminal to the RVXF motif previously shown to be important for binding to PP-1c isoforms [42,55]. (**D**) An *in vitro* Ni-NTA agarose-binding experiment, comparing the binding of wild-type PP-1c$\alpha$ (WT), PP-1c$\alpha$ A259R, PP-1c$\alpha$ K260D, PP-1c$\alpha$ R261S to His-tagged ASPP1$^{867–1090}$, ASPP2$^{905–1128}$ and iASPP$^{608–828}$. Approximately 5 $\mu$g of ASPP protein was bound to Ni-NTA resin for 1 h at 4 °C end-over-end. Resin was washed and 5 $\mu$g of wild-type PP-1c$\alpha$ or mutant PP-1c$\alpha$ was incubated with resin for an additional 1 h at 4 °C. After washing, bound protein was eluted by the addition of SDS/PAGE loading buffer, heated to 100 °C for 5 min and analysed by SDS/PAGE with Coomassie Blue staining.

results of the present study show (Figure 7) that the PP-1c phosphomimic mutation T311D completely abolished the ability of PP-1c to bind to ASPP1$^{867–1090}$, ASPP2$^{905–1128}$ and iASPP$^{608–828}$. SPR (surface plasmon resonance) experiments (Figure 8) also revealed that iASPP$^{608–828}$ binds to PP-1c$\alpha$ with a 5-fold higher affinity ($K_d = 26 \pm 0.4$ nM) compared with ASPP2$^{905–1128}$ ($K_d = 123 \pm 8$ nM). Significantly, a peptide corresponding to PP-1c$\alpha$ residues 301–330 alone was sufficient to bind to both iASPP$^{608–828}$ and ASPP2$^{905–1128}$, with a $K_d$ of $53 \pm 7$ nM and $136 \pm 8$ nM respectively. These apparent binding constants are comparable with RVXF-containing peptides derived from MYPT1 and the glycogen-targeting subunit $G_M$ [47,48]. This suggests that the C-terminus of PP-1c is essential for the high-affinity binding of PP-1c to the ASPP proteins. Additionally, iASPP binds with a higher affinity to the PP-1c C-terminal peptide compared with ASPP2, suggesting that iASPP and ASPP2 differentially interact with the PP-1c C-terminus. A detailed analysis of the iASPP and ASPP2 crystal structures [14,37] revealed no obvious differences between the two structures that could account for the differences in binding affinity to the PP-1c C-terminal peptide and we are currently investigating these interactions via NMR spectroscopy.

All three ASPP proteins contain a proline-rich region located N-terminal to the RVXF motif (Figure 1). In theory, the proline-rich region of the ASPP proteins may interact with its own SH3 domain and directly interfere with the binding of the PP-1c C-terminus. It has been shown previously that a construct of ASPP2 containing the proline-rich, ankyrin-repeat and SH3 domains weakened binding to NF-$\kappa$B, as compared with an ASPP2 construct containing only ankyrin-repeat and SH3 domains [49]. Full-length ASPP1 and iASPP bind directly to PP-1c in HeLa cells, which argues against a significant role for these proline-rich motifs to interfere with the binding to PP-1c (Figure 2).

### An alternative mechanism for PP-1c binding to iASPP

In parallel with the present study, Llanos et al. [28] have shown that mutations within the iASPP SH3 domain disrupt binding of iASPP to PP-1c; in particular, mutation of iASPP Phe$^{815}$ to an alanine residue causes a complete loss of binding to PP-1c. They identify a 'RNYF' motif (residues 812–815) within the iASPP SH3 domain that is proposed to be critical for interaction with PP-1c. However, the crystal structure of iASPP alone reveals that Phe$^{815}$ of iASPP is 100 % buried within the iASPP SH3 domain [50]. Furthermore, previous NMR studies have shown that mutation of the equivalent residue in the Fyn SH3 domain causes destabilization and misfolding of the entire SH3 domain [50]. It is unlikely that these residues comprise a true RVXF-like PP-1c-binding motif since they are not accessible to the phosphatase for binding. A more plausible explanation is that mutation of F815A destabilizes the entire SH3 domain, producing a non-functional domain. Structural collapse of the iASPP SH3 domain would prevent iASPP from interacting directly with the PxxPxR SH3-binding motif on the C-terminus of PP-1c.

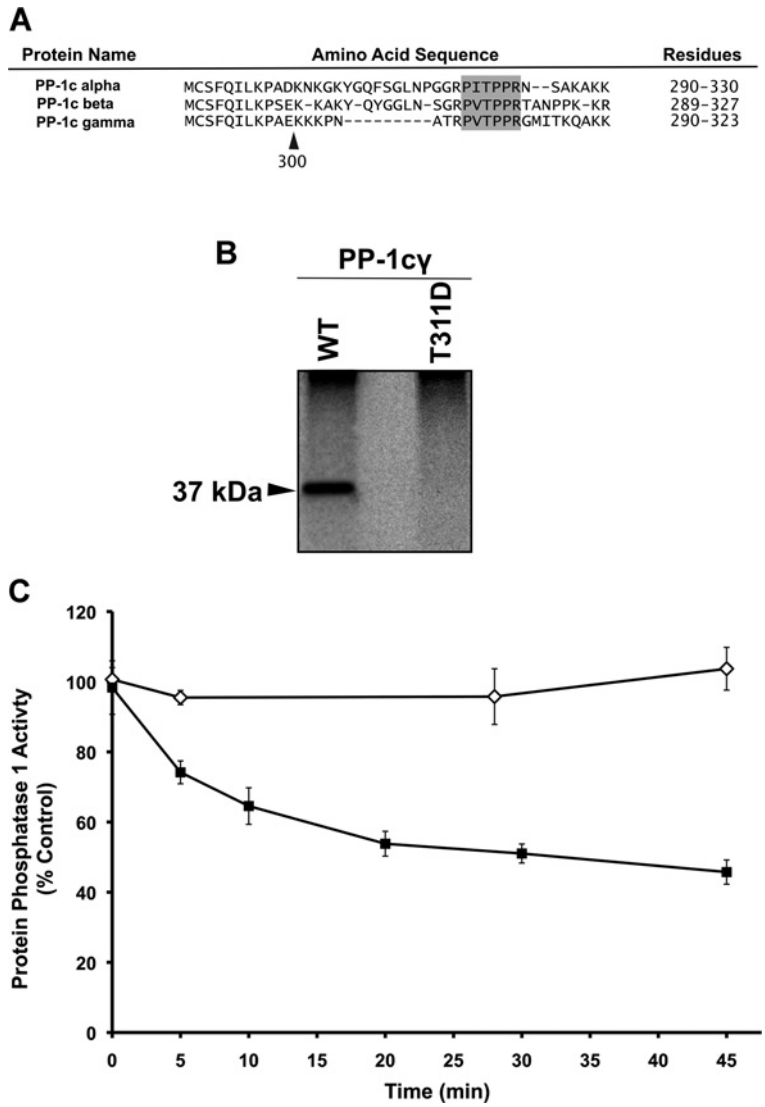


**Figure 6 The C-terminus of PP-1c contains a putative Px(T)PxR SH3-binding motif comprising the phosphorylation site for CDK2–cyclin A**

(**A**) A multiple sequence alignment of the C-termini of PP-1c isoforms $\alpha$, $\beta$ and $\gamma$ (UniProt numbers P62136, P62140 and P36873 respectively). The arrow indicates the residue 300 at which the PP-1c$\gamma$ (residues 1–300) construct was truncated. The shaded box highlights the canonical type-2 SH3-binding motif PxxPxR. (**B**) An autoradiograph of phosphorylated PP-1c$\gamma$ and hPP-1c$\gamma$ T311D. Proteins were phosphorylated for 30 min at 30 °C with CDK2–cyclin A (New England Biolabs) and [$\gamma$-$^{32}$P]ATP. WT, wild-type. (**C**) The effect of phosphorylation of wild-type PP-1c$\gamma$ (■) and PP-1c$\gamma$-T311D (◇) on enzymatic activity. The activity of both enzymes was determined using $^{32}$P-labelled phosphorylase *a* as the substrate. Values are means ± S.D. ($n = 3$).

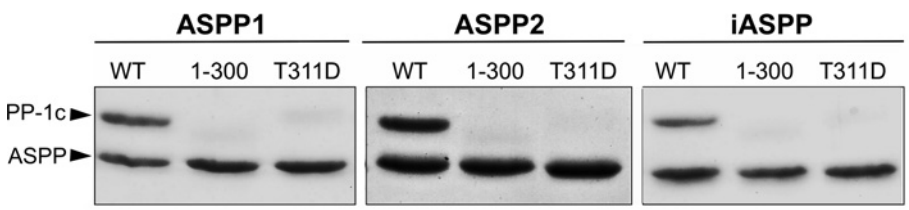


**Figure 7 Mutation or deletion of the PP-1c C-terminus abolishes the ability of PP-1c to bind to the ASPP proteins**

An *in vitro* Ni-NTA agarose-binding experiment comparing the binding of ASPP1$^{867–1090}$, ASPP2$^{905–1128}$ and iASPP$^{608–828}$ with full-length wild-type PP-1c$\gamma$, truncated PP-1c$\gamma$ (residues 1–300) and mutated PP-1c$\gamma$ T311D. Each ASPP construct (5 $\mu$g) was bound to Ni-NTA resin for 1 h at 4 °C end-over-end. Resin was washed and 5 $\mu$g of PP-1c$\gamma$ [WT represents wild-type PP-1c$\gamma$; 1–300 represents truncated PP-1c$\gamma^{1–300}$; and T311D represents the PP-1c$\gamma$ T311D single mutant] was incubated with ASPP-bound resin for an additional 1 h at 4 °C. After washing, bound protein was eluted by the addition of SDS/PAGE loading buffer, heated for 5 min at 100 °C and analysed by SDS/PAGE with Coomassie Blue staining.

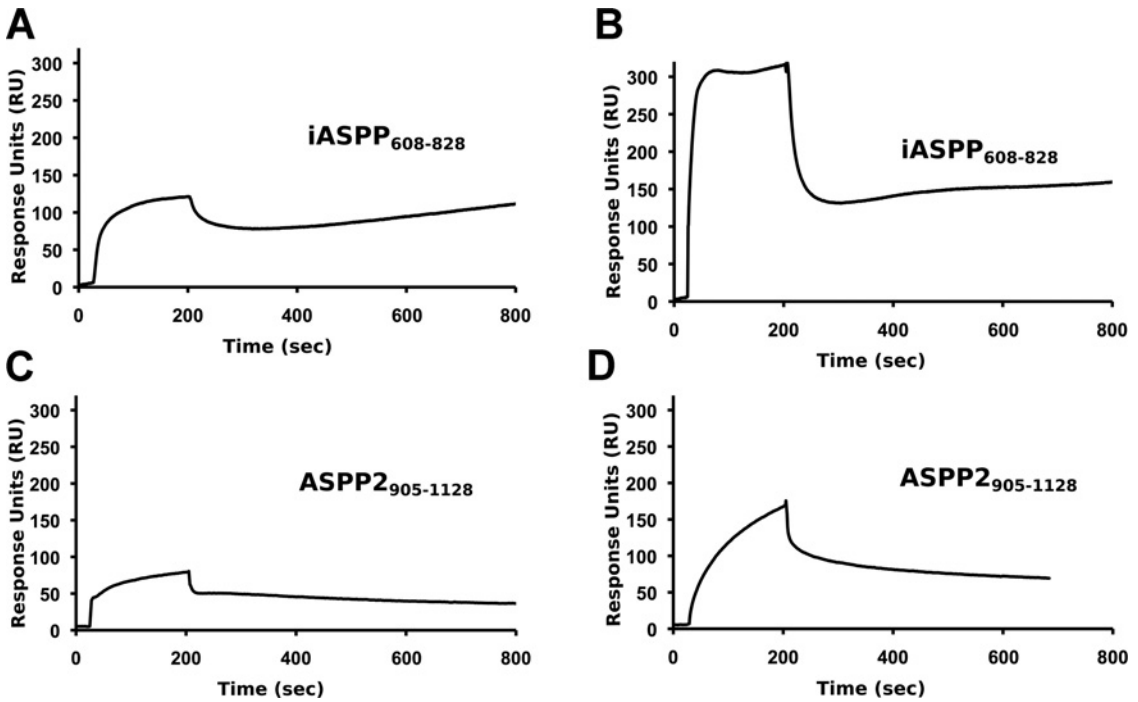


**Figure 8 Interaction of iASPP$^{608–828}$ and ASPP2$^{905–1128}$ with full-length PP-1c$\alpha$ and a C-terminal PP-1c peptide (PP-1c$\alpha$, residues 301–330)**

SPR (surface plasmon resonance) sensograms of the interaction of iASPP$^{608–828}$ and ASPP2$^{905–1128}$, with full-length PP-1c$\alpha$ (**A** and **B**) and a C-terminal PP-1c peptide corresponding to PP-1c$\alpha$ residues 301–330 (**C** and **D**). Approximately 0.3 $\mu$M solutions of iASPP and ASPP2 were immobilized on a CM5 sensor chip at 5 $\mu$l/min for 7 min. All lanes were blocked with 1 M ethanolamine. Kinetic analyses were performed by injecting either full-length PP-1c$\alpha$ or a C-terminal PP-1c peptide as an analyte in a titration curve of 5000–78.125 nM, performed in triplicate. The association/dissociation curve for each sample injection was fitted using BIAevaluation 3.2 analysis software using the kinetic analysis result wizard and a drifting baseline (1:1 Langmuir binding) model. A representative curve at 5000 nM is shown for each kinetic analysis.

On the basis of the results of the present study, we propose a model for how phosphorylation of the C-terminal tail of PP-1c may alter its interaction with its regulatory proteins, including the ASPP proteins. In normal dividing cells, the C-terminus of PP-1c is phosphorylated during M-phase, causing auto-inhibition of PP-1c, contributing to a high level of mitotic phosphoproteins that allow the cell to proceed through mitosis [1]. When phosphorylated, PP-1c cannot interact with the ASPP proteins and may therefore not be able to dephosphorylate p53. Lack of association with ASPP proteins may also alter the subcellular localization of PP-1c. When cells are damaged and CDK2 is not constitutively activated, then PP-1c may be slowly reactivated by auto-dephosphorylation of its C-terminal tail, at which point PP-1c is freer to associate with ASPP1 or ASPP2. However, in many cancer cells, iASPP is overexpressed and will probably compete with ASPP1 and ASPP2 for binding to PP-1c and p53.

### A functional role for PP-1c–ASPP interactions in differential scaffolding of the p53 tumour suppressor

In order to understand the significance of the novel iASPP–PP-1c and ASPP1–PP-1c interactions, a key question was whether ASPP proteins can bind to both PP-1c and p53 in a trimeric complex. Previously, Helps et al. [27] showed that GST-tagged p53BP2 (ASPP2) does not bind to both p53 and PP-1c simultaneously. To address this question we first analysed using gel-filtration chromatography whether PP-1c and p53 could bind directly, using a p53 construct that contains both the N-terminal transactivation domain and the central DNA-binding domain (p53$^{2–293}$). We show that p53 and PP-1c do not bind directly to one another (Supplementary Figure S2 at http://www.biochemj.org/bj/449/bj4490649add.htm). Subsequently, we carried out distinct gel-filtration chromatography experiments with PP-1c, the ASPP proteins and p53$^{2–293}$. Consistent with the Helps et al. [27] data, we show that ASPP2 does not form a trimeric complex with p53 and PP-1c (Supplementary Figure S2). However, interestingly iASPP readily forms a stable complex with p53 and PP-1c (Supplementary Figure S3 at http://www.biochemj.org/bj/449/bj4490649add.htm).

### The potential role for ASPP–PP-1c complexes in the regulation of p53 activation and their role in cancer

A question that arises from the present study is whether the formation of a PP-1c–iASPP–p53 complex will alter the phosphorylation state of p53. Previously, PP-1c was shown to dephosphorylate p53 on phosphorylated Ser$^{15}$ and Ser$^{37}$ residues within the N-terminal transactivation domain [51]. Phosphorylation of p53 on Ser$^{15}$ is an important step towards the activation of p53 and induction of cell-cycle arrest or apoptosis [52]. We hypothesize that formation of the PP-1c–iASPP–p53 trimeric complex may promote the specific dephosphorylation of p53 by PP-1c at these key residues. Further experiments are required to fully understand the full spectrum of site-specific dephosphorylation of p53 when assembling with iASPP and PP-1c in a trimeric complex.

ASPP1 and ASPP2 protein expression is often down-regulated in many forms of cancer that express wild-type p53. For example, ASPP1 and ASPP2 promoters are hypermethylated in HBV (hepatitis B virus)-positive HCC (hepatocellular carcinoma), leading to decreased ASPP1 and ASPP2 expression and early development of HCC [53]. Approximately 30 % of HCC contain

p53 mutations, and methylation of ASPP1 and ASPP2 was more frequent in cancers that expressed wild-type p53. On the other hand, iASPP is overexpressed in many forms of cancer that typically express wild-type p53 and normal levels of ASPP2. Overexpression of iASPP in many forms of cancer may lead to hypophosphorylated p53 via the PP-1c–iASPP–p53 trimeric complex and ultimately lead to the inhibition of apoptotic activity of p53.

Overexpression of iASPP observed in some forms of cancer may in fact be one way to override wild-type p53 and disrupt the p53 apoptotic pathway. siRNA (small interfering RNA)-mediated down regulation of iASPP in hepatocellular cancer cells leads to a decrease in cell proliferation and tumour growth [54]. Therefore the iASPP–PP-1c complex is a potentially valuable molecular target for development of cancer therapies. For example, by understanding the key molecular interactions between PP-1c, ASPP proteins and p53, we can develop sensitive screening methodologies to identify novel lead compounds that may specifically disrupt either p53 or PP-1c binding to iASPP.

## AUTHOR CONTRIBUTION

Tamara Skene-Arnold contributed Figures 1, 3, 4, 5(C), 5(D), 6(A), 7 and 8, and all Supplementary Figures, designed experiments, analysed data and wrote the paper with Charles Holmes. Hue Anh Luu carried out mutagenesis of PP-1c$\alpha$ mutants A259R, K260D and R261S and assisted Tamara Skene-Arnold with experiments. Glen Uhrig, Veerle De Wever and Mhairi Nimick performed the experiments for Figure 2. Jason Maynes generated the ASPP2–PP-1c dimeric complex model (Figures 5A and 5B). Andrea Fong designed and performed experiments for Figures 6(B) and 6(C). Michael James supervised Jason Maynes and assisted development of complex models. Laura Trinkle-Mulcahy designed, carried out and analysed SILAC experiments (Table 1). Greg Moorhead supervised the experiments carried out by Glen Uhrig, Veerle De Wever and Mhairi Nimick. Charles Holmes is the corresponding author, supervised the experiments carried out by Tamara Skene-Arnold, Hue Anh Luu and Andrea Fong, and wrote the paper with Tamara Skene-Arnold.

## ACKNOWLEDGEMENTS

We thank Dr Xin Lu (Ludwig Institute for Cancer Research, Oxford, U.K.) for providing the full-length constructs for ASPP2 and iASPP and Dr D. Elliot (University of Newcastle, Newcastle, U.K.) for providing the full-length human ASPP1 construct. We also thank Jonathan Pan and Peter Hwang (Sykes Laboratory, University of Alberta, Edmonton, AB, Canada) for producing the PP-1c$\alpha$ peptide. We would especially like to thank Dr Jody Groenendyk for her invaluable assistance with the surface plasmon resonance experiments.

## FUNDING

Financial support was provided by an Alberta Ingenuity Fund Studentship (to T.D.S.-A.), the Canadian Institutes of Health Research [grant numbers MOP-13607 (to C.F.B.H.) and MOP-37770 (to M.N.G.J.)] and the Natural Sciences and Engineering Council Canada (to G.B.M.).

## REFERENCES

1 Olsen, J. V., Vermeulen, M. V., Satamaria, A., Kumar, C., Miller, M. L., Jensen, L. J., Gnad, F., Cox, J., Jensen, T. S., Nigg, E. A. et al. (2010) Quantitative phosphoproteomics reveals widespread full phosphorylation site occupancy during mitosis. Sci. Signaling **3**, 1–15
2 Ceulemans, H. and Bollen, M. (2004) Functional diversity of protein phosphatase-1, a cellular economizer and reset button. Phys. Rev. **84**, 1–39
3 Hendrickx, A., Beullens, M., Ceulemans, H., Abt, T. D., Van Eynde, A., Nicolaescu, E., Lesage, B. and Bollen, M. (2009) Docking motif-guided mapping of the interactome of protein phosphatase-1. Chem. Biol. **16**, 365–371
4 Peti, W., Nairn, A. C. and Page, R. (2012) Structural basis for protein phosphatase 1 regulation and specificity. FEBS Lett., doi:10.1111/j.1742-4658.2012.08509.x.
5 Allen, P. B., Ouimet, C. C. and Greengard, P. (1997) Spinophilin, a novel protein phosphatase 1 binding protein localized to dendritic spines. Proc. Natl. Acad. Sci. U.S.A. **94**, 9956–9961
6 Terrak, M., Kerff, F., Langsetmo, K., Tao, T. and Dominguez, R. (2004) Structural basis of protein phosphatase 1 regulation. Nature **429**, 780–784
7 Egloff, M. P., Johnson, D. F., Moorhead, G., Cohen, P. T. W., Cohen, P. and Barford, D. (1997) Structural basis for the recognition of regulatory subunits by the catalytic subunit of protein phosphatase 1. EMBO J. **16**, 1876–1887
8 Wakula, P., Beullens, M., Ceulemans, H., Stalmans, W. and Bollen, M. (2003) Degeneracy and function of the ubiquitous RVXF-motif that mediates binding of protein phosphatase-1. J. Biol. Chem. **278**, 18817–18823
9 Ulke-Lemmee, A., Trinkle-Mulcahy, L., Chaulk, S., Bernstein, N. K., Morrice, N., Glover, M. and Moorhead, G. B. G. (2007) The nuclear PP1 interacting protein ZAP3 (ZAP) is a putative nucleoside kinase that complexes with SAM68, CIA, NF110/45, and HNRNP-G. Biochim. Biophys. Acta **283**, 398–404
10 Johnson, D. F., Moorhead, G., Caudwell, F. B., Cohen, P., Chen, Y. H., Chen, M. X. and Cohen, P. T. W. (1996) Identification of protein-phosphatase-1 binding domains on glycogen and myofibrillar targeting subunits. Eur. J. Biochem. **239**, 317–325
11 Trigiante, G. and Xin, L. (2006) ASPPs and cancer. Nat. Cancer Rev. **6**, 217–226
12 Bergamaschi, D., Sameuls, Y., Sullivan, A., Zvelebil, M., Breyssens, H., Bisso, A., Del Sal, G., Syed, N., Smith, P., Gasco, M. et al. (2006) iASPP preferentially binds to p53 proline-rich region and modulates apoptotic function of codon 72-polymorphic p53. Nat. Genet. **38**, 1133–1141
13 Sameuls-Lev, Y., O'Connor, D., Bergamaschi, D., Trigiante, G., Hsieh, J. K., Zhong, S., Campargue, I., Naumovski, L., Crook, T. and Lu, X. (2001) ASPP proteins specifically stimulate the apoptotic function of p53. Mol. Cell **8**, 781–794
14 Gorina, S. and Pavletich, N. P. (1996) Structure of p53 tumor suppressor bound to ankyrin and SH3 domains of p53BP2. Science **274**, 1001–1005
15 Cho, Y., Gorina, S., Jeffrey, P. D. and Pavletich, N. P. (1994) Crystal structure of a p53 tumor suppressor–DNA complex: understanding tumorgenic mutations. Science **265**, 346–355
16 Thukral, S. K., Blain, G. C., Chang, K. K. H. and Fields, S. (1994) Distinct residues of human p53 implicated in binding to DNA, simian virus 40 large T antigen, 53BP1 and 53BP2. Mol. Cell. Biol. **14**, 8315–8321
17 Yang, J. P., Hori, M., Sanda, T. and Okamoto, T. (1999) Identification of a novel inhibitor of nuclear factor-$\kappa$B, relA-associated inhibitor. J. Biol. Chem. **274**, 15662–15670
18 Zhang, X., Wang, M., Zhou, S., Chen, S. and Wang, J. (2005) The expression of iASPP in acute leukemias. Leuk. Res. **29**, 179–183
19 Laska, M. J., Vogel, U. B., Jensen, U. B. and Nexo, B. A. (2010) p53 and PPP1R13L (alias iASPP or RAI) form a feedback loop to regulate genotoxic stress responses. Biochem. Biophys. Acta **1800**, 1231–1240
20 Bergamaschi, D., Sameuls, Y., O'Neil, N. J., Trigiante, G., Crook, T., Hsieh, J. K., O'Connor, D. J., Zhong, S., Campargue, I., Tomlinson, M. L. et al. (2003) iASPP oncoprotein is a key inhibitor of p53 conserved from worm to human. Nat. Genet. **33**, 162–167
21 Yang, J. P., Hori, M., Takahashi, N., Kawabe, T., Kato, H. and Okamoto, T. (1999) NF-$\kappa$B subunit p65 binds to 53BP2 and inhibits cell death induced by 53BP2. Oncogene **18**, 5177–5186
22 Cao, Y., Hamada, T., Matsui, T., Date, T. and Iwabuchi, K. (2004) Hepatitis C virus core protein interacts with p53-binding protein, 53BP2/Bbp/ASPP2, and inhibits p53-mediated apoptosis. Biochem. Biophys. Res. Commun. **315**, 788–795
23 Katz, C., Benyamini, H., Rotern, S., Lebendiker, M., Danieli, T., Iosub, A., Refaely, H., Dines, M., Bronner, V., Bravman, T. et al. (2008) Molecular basis of the interaction between the antiapoptotic family proteins and the proapoptotic protein ASPP2. Proc. Natl. Acad. Sci. U.S.A. **105**, 12277–12282
24 Espanel, X. and Sudol, M. (2001) Yes-associated protein and p53-binding protein-2 interact through their WW and SH3 domains. J. Biol. Chem. **276**, 14514–14523
25 Vigneron, A. M., Ludwig, R. L. and Vousden, K. H. (2010) Cytoplasmic ASPP1 inhibits apoptosis through the control of YAP. Genes Dev. **24**, 2430–2439
26 Aylon, Y., Ofir-Rosenfield, Y., Yabuta, N., Lapi, E., Nojima, H., Lui, X. and Oren, M. (2010) The Lats2 tumor suppressor augments p53-mediated apoptosis by promoting the nuclear proapoptotic function of ASPP1. Genes Dev. **24**, 2420–2429
27 Helps, N. R., Barker, H. M., Elledge, S. J. and Cohen, P. T. W. (1995) Protein phosphatase 1 interacts with p53BP2, a protein which binds to the tumour suppressor p53. FEBS Lett. **377**, 295–300
28 Llanos, S., Royer, C., Lu, M., Bergamaschi, D., Lee, W. H. and Lu, X. (2011) The inhibitory member of the apoptosis stimulating proteins of p53 family (iASPP) interacts with protein phosphatase (PP1) via a non-canonical binding motif. J. Biol. Chem. **286**, 43039–43044
29 Boland, M. P., Smillie, M. A., Chen, D. Z. X. and Holmes, C. F. B. (1993) A unified bioscreen for the detection of diarrhetic shellfish toxins and microcystins in marine and freshwater environments. Toxicon **31**, 1393–1405
30 Thornton, J. K., Dalgleish, C., Venables, J. P., Sergeant, K. A., Ehrmann, I. E., Lu, X., Saunders, P. T. K. and Elliott, D. J. (2006) The tumour-suppressor protein ASPP1 is nuclear in human germ cells and can modulate ratios of CD44 exon V5 spliced isoforms *in vivo*. Oncogene **25**, 3104–3112

31 Moorhead, G. B., Haystead, T. A. and MacKintosh, C. (2007) Synthesis and use of protein phosphatase affinity matrices microcystin-sepharose and microcystin-biotin-sepharose. Methods Mol. Biol. **365**, 39–45

32 Moorhead, G., MacKintosh, R. W., Morrice, N., Gallagher, T. and MacKintosh, C. (1994) Purification of type 1 protein (serine/threonine) phosphatases by microcystin–Sepharose affinity chromatography. FEBS Lett. **356**, 46–50

33 Moorhead, G. B. G., Trinkle-Mulcahy, L., Nimick, M., De Wever, V., Campbell, D. G., Gourlay, R., Lam, Y. W. and Lamond, A. I. (2008) Displacement affinity chromatography of protein phosphatase one (PP-1) complexes. BMC Biochem. **9**, 28

34 Maynes, J. T., Perreault, K. R., Cherney, M. M., Luu, H. A., James, M. N. G. and Holmes, C. F. B. (2004) Crystal structure and mutagenesis of a protein phosphatase-1:calcineurin hybrid elucidate the role of $\beta$12–$\beta$13 loop in inhibitor binding. J. Biol. Chem. **274**, 43198–43206

35 An, J. and Carmichael, W. W. (1994) Use of a colourmetric protein phosphatase inhibition assay and enzyme linked immunosorbent assay for the study of microcystins and nodularins. Toxicon **32**, 1495–1507

36 McCready, T. L., Islam, B. F., Schmitz, F. J., Luu, H. A., Dawson, J. F. and Holmes, C. F. B. (2000) Inhibition of protein phosphatase-1 by clavosines A and B, novel members of the calyculin family of toxins. J. Biol. Chem. **275**, 4192–4198

37 Robinson, R. A., Lu, X., Jones, E. Y. and Siebold, C. (2008) Biochemical and structural studies of ASPP proteins reveal differential binding to p53, p63, and p73. Structure **16**, 259–268

38 Trinkle-Mulcahy, L., Andersen, J., Lam, Y. W., Moorhead, G., Mann, M. and Lamond, A. I. (2006) Repo-Man recruits PP1$\gamma$ to chromatin and is essential for cell viability. J. Cell Biol. **172**, 679–692

39 Trinkle-Mulcahy, L., Boulon, S., Lam, Y. W., Urcia, R., Boisvert, F. M., Vandermoere, F., Morrice, N. A., Swift, S., Rothbauer, U., Leonhardt, H. and Lamond, A. I. (2008) Identifying specific protein interaction partners using quantitative mass spectrometry and bead proteomes. J. Cell Biol. **183**, 223–239

40 Berndt, N. (1998) Control of PP1 activity through phosphorylation by cyclin-dependent kinases. Methods Mol. Biol. **93**, 67–77

41 MacKintosh, C. (1993) Assay Phosphorylation: a Practical Approach. Oxford University Press, Oxford

42 Carmody, L. C., Baucum, A. J., Bass, M. A. and Colbran, R. J. (2008) Selective targeting of the $\gamma$1 isoform of protein phosphatase 1 to F-actin in intact cells requires multiple domains in spinophilin and neurabin. FASEB J. **22**, 1660–1671

43 Hurley, T. D., Yang, J., Goodwin, K. D., Zou, Q., Cortese, M., Dunker, K. and DePaoli-Roach, A. A. (2007) Structural basis for regulation of protein phosphatase 1 by inhibitor-2. J. Biol. Chem. **282**, 28874–28883

44 Ragusa, M. J., Dancheck, B., Critton, D. A., Nairn, A. C., Page, R. and Peti, W. (2010) Crystal structure of a complex between protein phosphatase 1$\alpha$ (PP1), the PP1 binding and PDZ domains of spinophilin and the small natural molecular toxin nodularin-R. Nat. Struct. Biol. **17**, 459–464

45 Dohadwala, M., da Cruz e Silva, E. F., Hall, F. L., Williams, R. T., Carbonaro-Hall, D. A., Nairn, A. C., Greengard, P. and Berndt, N. (1994) Phosphorylation and inactivation of protein phosphatase 1 by cyclin-dependent kinases. Proc. Natl. Acad. Sci. U.S.A. **91**, 6048–6412

46 Kwon, Y. G., Lee, S. Y., Choi, Y., Greengard, P. and Nairn, A. C. (1997) Cell cycle-dependent phosphorylation of mammalian protein phosphatase 1 by cdc2 kinase. Proc. Natl. Acad. Sci. U.S.A. **94**, 2168–2173

47 Toth, A., Kiss, E., Herberg, F. W., Gergely, P., Hartshorne, D. J. and Erdodi, F. (2000) Study of the subunit interactions in myosin phosphatase by surface plasmon resonance. Eur. J. Biochem. **267**, 1687–1697

48 Schillace, R. V. and Scott, J. D. (1999) Association of the type 1 protein phosphatase PP1 with the A-kinase anchoring protien AKAP220. Curr. Biol. **9**, 321–324

49 Rotem, S., Katz, C., Benyamini, H., Lebendiker, M., Veprintsev, D., Rudiger, S., Danieli, T. and Friedler, A. (2008) The structure and interactions of the proline-rich domain of ASPP2. J. Biol. Chem. **283**, 18890–18899

50 Northey, J., Di Nardo, A. A. and Davidson, A. R. (2002) Hydrophobic core packing in the SH3 domain folding transition state. Nat. Struct. Biol. **9**, 126–130

51 Li, D. W. C., Liu, J. P., Schmid, P. C., Schlosser, R., Feng, H., Liu, W. B., Yan, Q., Gong, L., Sun, S. M., Deng, M. and Liu, Y. (2006) Protein serine/threonine phosphatase-1 dephosphorylates p53 at $Ser^{15}$ and $Ser^{37}$ to modulate its transcriptional and apoptotic activities. Oncogene **25**, 3006–3022

52 Fiscella, M., Ullrich, S. J., Zambrano, N., Shields, M. T., Lin, D., Lees-Miller, S. P., Anderson, C. W., Mercer, W. E. and Appella, E. (1993) Mutation of the serine 15 phosphorylation site of human p53 reduces the ability of p53 to inhibit cell cycle progression. Oncogene **8**, 1519–1528

53 Zhao, J., Wu, G., Lu, B., Liang, A., Cao, L., Tong, X., Lu, X., Wu, M. and Guo, Y. (2010) Epigenetic silence of ankyrin-repeat-containing, SH3-domain-containing, and proline-rich-region-containing protein 1 (ASPP1) and ASPP2 genes promotes tumor growth in hepatitis B virus-positive hepatocellular carcinoma. Hepatology **51**, 142–153

54 Lin, B. L., Xie, D. Y., Xie, S. B., Xie, J. Q., Zhang, X. H., Zhang, Y. F. and Gao, Z. L. (2011) Down-regulation of iASPP in human hepatocellular carcinoma cells inhibits cell proliferation and tumor growth. Neoplasia **58**, 205–210

55 Carmody, L. C., Bauman, P. A., Bass, M. A., Mavila, N., DePaoli-Roach, A. A. and Colbran, R. J. (2004) A protein phosphatase-1$\gamma$1 isoform selectivity determinant in dendritic spine-associated neurabin. J. Biol. Chem. **279**, 21714–21723


Received 29 March 2012/17 September 2012; accepted 23 October 2012
Published as BJ Immediate Publication 23 October 2012, doi:10.1042/BJ20120506

Biochem. J. (2013) **449**, 649–659 (Printed in Great Britain) doi:10.1042/BJ20120506

online data

## SUPPLEMENTARY ONLINE DATA

# Molecular mechanisms underlying the interaction of protein phosphatase-1c with ASPP proteins

Tamara D. SKENE-ARNOLD*, Hue Anh LUU*, R. Glen UHRIG†, Veerle DE WEVER†, Mhairi NIMICK†, Jason MAYNES‡, Andrea FONG*, Michael N. G. JAMES*, Laura TRINKLE-MULCAHY§, Greg B. MOORHEAD† and Charles F. B. HOLMES*[1]

*Department of Biochemistry, 3-37 Medical Sciences Building, School of Translational Medicine, Faculty of Medicine and Dentistry, University of Alberta, Edmonton, Canada, T6G 2H7, †Department of Biological Sciences, University of Calgary, AB, Calgary, Canada, T2N 1N4, ‡Department of Paediatric Anaesthesia and Molecular Structure and Function, Hospital for Sick Children/SickKids Research Institute, Faculty of Medicine, University of Toronto, Toronto, ON, Canada, M5G 1X8, and §Department of Cellular and Molecular Medicine, University of Ottawa, Ottawa, ON, Canada, KIH 8MS

## MATERIALS AND METHODS

### Mutagenesis of PP-1c$\gamma$ (T311D) and PP-1c$\alpha$ (PP-1c$\alpha$ A259R, K260D and R261S)

Mutagenesis of PP-1c was carried out using QuikChange® site-directed mutagenesis (Stratagene) as described previously [1]. All PP-1c$\gamma$ mutants were validated by DNA sequencing. PP-1c mutants were subsequently transformed into either DH5$\alpha$ cells for long-term storage or C41 DE3 cells (Lucigen) for protein expression. The phospho-mimic mutant PP-1c$\alpha$ (T320D) was very poorly expressed, whereas PP-1c$\gamma$ (T311D) was expressed well, yielding milligram quantities of enzyme. The specific activities of wild-type PP-1c$\gamma$ and the T311D mutant were equivalent (25.7 and 27.1 units/mg respectively). The PP-1c$\gamma$ mutants (T311D) and PP-1c$\alpha$ mutants (A259R, K260D and R261S) were purified as described above for wild-type PP-1c$\gamma$.

### Molecular cloning and expression of full-length ASPP1

A full-length construct comprising human ASPP1 (a gift from Dr D. Elliott, University of Newcastle, Newcastle, U.K.) was cloned directly into pET101 via directional TOPO expression (Invitrogen). Subsequent site-directed mutation of the ASPP1 RVRF PP-1c-docking motif to RARA was performed using QuikChange® site-directed mutagenesis. Each construct was initially transformed into TOP10 *E. coli* cells (Invitrogen), followed by subsequent transformation in the expression *E. coli* strain BL21 (DE3) Star (Invitrogen). Both wild-type and mutated (RARA) ASPP1 constructs were expressed and purified using the same conditions. Each ASPP1 bacterial culture was induced at $D_{600} = 0.6$ with 0.1 mM IPTG and grown for 18 h at 28 °C. Protein-expressing bacteria were pelleted using a SH3000 Sorvall rotor at 1300 ***g*** for 30 min, re-suspended in buffer C [25 mM Tris/HCl (pH 7.5), 150 mM NaCl, 10 mM imidazole with 0.5 mM PMSF and 0.5 mM benzamidine] containing 5 $\mu$g/ml leupeptin, snap frozen and stored at − 80 °C until used. Bacteria were lysed using a French Press at 10000 psi (1 psi = 6.9 kPa). Crude lysates were clarified via ultracentrifugation at 35000 rev./min for 30 min at 4 °C using a Beckman Ti45 rotor. Clarified supernatants were incubated with Ni-NTA (Qiagen) for 1 h end-over-end at 4 °C. Ni-NTA matrices were washed with 100 column volumes of buffer D [25 mM Tris/HCl (pH 7.5), 1 M NaCl, 30 mM imidazole, 0.1 % Tween 20, 0.5 mM PMSF and 0.5 mM benzamidine], followed by 20 column volumes of buffer C. Each ASPP1 protein was eluted using buffer C containing 300 mM imidazole. ASPP1 fractions were concentrated and chromatographically separated on Superose-12 HR 10/30 (Pharmacia) pre-equilibrated in buffer E [25 mM Tris/HCl (pH 7.5), 150 mM NaCl, 5 % glycerol, 0.1 mM EDTA and 0.1 mM EGTA].

### Molecular modelling of the complex between PP-1c and ASPP2 (p53BP2)

The co-ordinates for PP-1c$\beta$ were taken from the PP-1c$\beta$–MYPT-1 complex (PDB code 1S70) [2] and the co-ordinates for the p53–ASPP2 complex were taken from PDB code 1YCS [3]. The ankyrin-repeat domains of ASPP2 were aligned with equivalent regions of MYPT-1 using the program DALI (http://protein.hbu.cn:83/fssp/www.ebi.ac.uk/dali/index.html) to give a probable method of interaction between PP-1c and ASPP2. The model underwent a round of simulated annealing to remove any bias from the starting X-ray crystal structures before undergoing ten rounds of rigid-body refinement and then ten rounds of torsion-angle refinement using the program CNS [4]. The target energy function for minimization used by CNS was based solely on stereochemistry, bonding and non-bonding interactions (no crystallographic information). The validity of the stereochemistry of the resulting model was confirmed using the programs WHATCHECK [5] and PROCHECK [6]. All Figures were created using the program PyMOL (http://www.pymol.org).

### Surface plasmon resonance

Interactions between PP-1c and the ASPP proteins (iASPP$^{608–828}$ and ASPP$^{2905–1128}$) were monitored by surface plasmon resonance using the Biacore 3000 biosensor instrument. A CM5 sensor chip was activated by injecting 35 $\mu$l of a 1:1 mixture of *N*-hydroxysuccinimide and *N*-ethyl-*N*′-(3-dimethylaminopropyl)-carbodiimide hydrochloride at 5 $\mu$l/min. The iASPP$^{608–828}$ or ASPP$^{2905–1128}$ constructs (35 $\mu$M) were diluted in 10 mM sodium acetate (pH 5) and immobilized on lanes 2 and 4 respectively at 5 $\mu$l/min until the protein was well coupled [∼1300–1500 RU (relative units)]. Lanes 1 and 3 were not coupled with protein and were instead used as control lanes. All lanes were then blocked with 1 M ethanolamine, pH 8.5 (35 $\mu$l) at 5 $\mu$l/min. Kinetic analyses were performed at 25 °C using running buffer [10 mM Hepes (pH 7.5), 150 mM NaCl, 0.005 % Tween 20 and 0.5 mM $MnCl_2$] at a flow rate of 30 $\mu$l/min. Full-length wild-type PP-1c$\alpha$ or a C-terminal PP-1c$\alpha$ peptide was used as the analyte in a titration curve of 5000–78.125 nM, performed in triplicate. Each sample was injected at 30 $\mu$l/min, 90 $\mu$l total

[1] To whom correspondence should be addressed (email Charles.holmes@ualberta.ca).

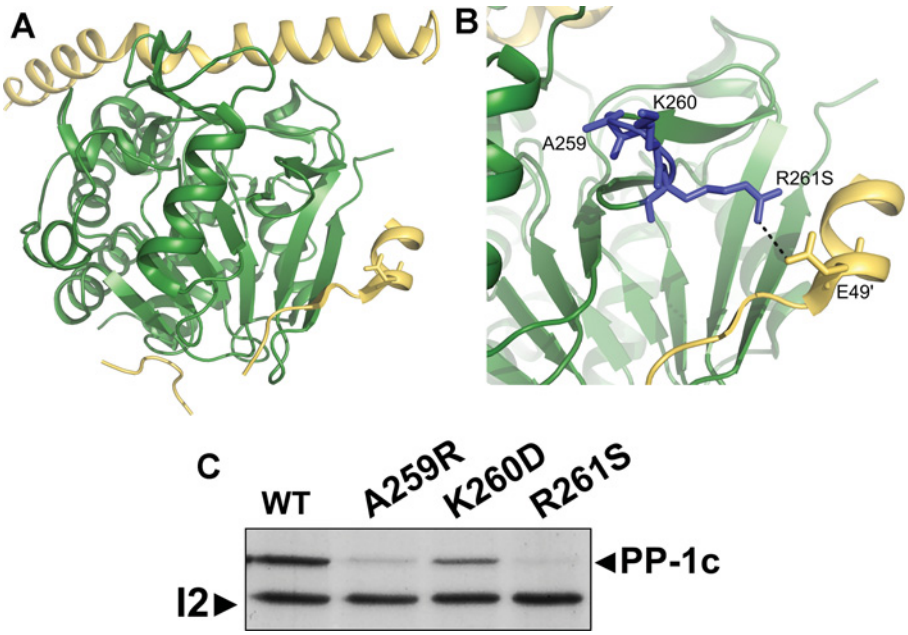


**Figure S1 Inhibitor-2 interacts with PP-1cα residues Ala$^{259}$ and Agr$^{261}$**

(**A** and **B**) The crystal structure of Inhibitor-2 bound to PP-1c (PDB code 2O8A) [7] suggests PP-1c residue Arg$^{261}$ may be important for binding. The colour scheme is as follows: PP-1c, green and Inhibitor-2, yellow. Ala$^{259}$, Lys$^{260}$ and Arg$^{261}$ of PP-1c are shown as blue sticks. (**C**) An *in vitro* Ni-NTA agarose-binding experiment comparing the binding of His-tagged Inhibitor-2 (I2) to PP-1cα A259R, K260D and R261S mutants respectively. Inhibitor-2 was incubated with Ni-NTA for 1 h at 4 °C end-over-end. Resin was washed with binding buffer and 5 μg of each PP-1c construct was added to each sample and incubated end-over-end for an additional 1 h at 4 °C. After washing, bound protein was eluted with SDS/PAGE loading buffer and boiled at 100 °C for 5 min. Eluted protein was analysed by SDS/PAGE with Coomassie Blue staining. WT, wild-type.

volume, followed by a 15 min dissociation time. Lanes were regenerated by injecting 15 μl of 0.2 % SDS diluted in running buffer, followed by a 2 min stabilization time. PP-1cα or the PP-1c peptide was simultaneously passed over the control lane to determine non-specific binding and the baseline was subtracted from the lane containing either immobilized iASPP or ASPP2. A representative curve at 5000 nM is shown for each kinetic analysis. The association/dissociation curve for each sample injection was fitted using BIAevaluation 3.2 analysis program (BIAcore control software, 3.2; Biacore) using the kinetic assay result wizard and a drifting baseline (1:1 Langmuir binding) model.

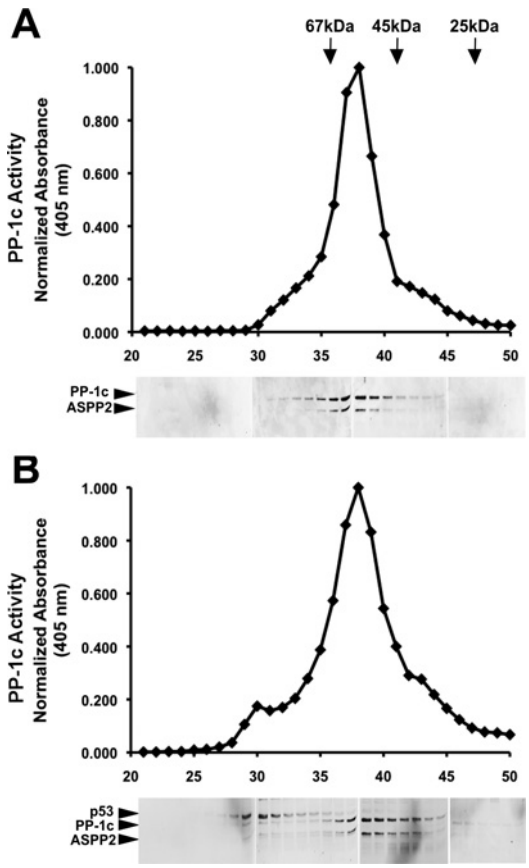


**Figure S2 ASPP2, PP-1c and p53 do not form a trimeric complex**

PP-1c$\alpha$ was incubated together with only ASPP2, or with both ASPP2 and p53$^{2-293}$ for 45 min at 30 °C. Samples were loaded on to a pre-equilibrated Superdex 75 10/30 gel-filtration column. Protein was eluted at 0.1 ml/min and 250 $\mu$l fractions were collected. Fractions from each gel-filtration run were measured for phosphatase activity using the pNPP phosphatase assay to determine where PP-1c elutes from the column. PP-1c$\alpha$ forms a dimeric complex with ASPP2 (**A**), but does not form a trimeric complex with both ASPP2 and p53 (**B**).

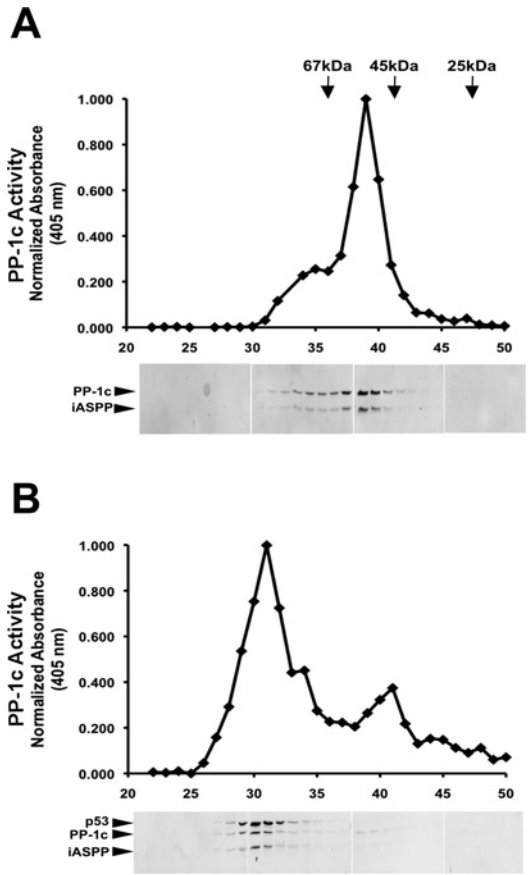


**Figure S3 iASPP forms a stable trimeric complex with p53 and PP-1c**

PP-1c$\alpha$ was incubated together with only iASPP, or with both iASPP and p53$^{2-293}$, for 45 min at 30 °C. Samples were loaded on to a pre-equilibrated Superdex 75 10/30 gel-filtration column. Protein was eluted at 0.1 ml/min and 250 $\mu$l fractions were collected. Fractions from each gel-filtration run were measured for phosphatase activity using the pNPP phosphatase assay to determine where PP-1c elutes from the column. iASPP readily forms a dimeric complex with PP-1c$\alpha$ (**A**) and also forms a stable complex with both p53 and PP-1c$\alpha$ (**B**).

## REFERENCES


1 McCready, T. L., Islam, B. F., Schmitz, F. J., Luu, H. A., Dawson, J. F. and Holmes, C. F. B. (2000) Inhibition of protein phosphatase-1 by clavosines A and B, novel members of the calyculin family of toxins. J. Biol. Chem. **275**, 4192–4198

2 Terrak, M., Kerff, F., Langsetmo, K., Tao, T. and Dominguez, R. (2004) Structural basis of protein phosphatase 1 regulation. Nature **429**, 780–784

3 Gorina, S. and Pavletich, N. P. (1996) Structure of p53 tumor suppressor bound to the ankyrin and SH3 domains of 53BP2. Science **274**, 1001–1005

4 Brunger, A. T., Adams, P. D., Clore, G. M., DeLano, W. L., Gros, P., Grosse-Kunstleve, R. W., Jiang, J. S., Kuszewski, J., Nilges, M., Parmu, N. S. et al. (1998) Crystallography and NMR system: a new software suite for macromolecular structure determination. Acta Crystallogr. Sect. D Biol. Crystallogr. **54**, 905–921

5 Hooft, R. W. W., Vriend, G., Sander, C. and Abola, E. E. (1996) Errors in protein structures. Nature **382**, 272

6 Laskowski, R. A., McArthur, M. W., Moss, D. S. and Thorton, J. M. (1993) PROCHECK: a program to check the stereochemical quality of protein structures. J. Appl. Cryst. **26**, 282–291

7 Hurley, T. D., Yang, J., Goodwin, K. D., Zou, Q., Cortese, M., Dunker, K. and DePaoli-Roach, A. A. (2007) Structural basis for regulation of protein phosphatase 1 by inhibitor-2. J. Biol. Chem. **282**, 28874–28883


Received 29 March 2012/17 September 2012; accepted 23 October 2012
Published as BJ Immediate Publication 23 October 2012, doi:10.1042/BJ20120506